Lasers in Manufacturing Conference 2025

Evaluation of the influence of the dynamics of the melt in the cutting kerf on the formation of burr during laser cutting with in-situ high-speed imaging

Sven Thomas[a,b*], Sem Massa[a], Max Rettenmeier[a,b], Steffen Wagenmann[c], Tim Hesse[a], Nicolai Speker[a], Christian Hagenlocher[d], Thomas Graf[b,d]

[a]*TRUMPF Laser- und Systemtechnik SE, Johann-Maus-Str. 2, 71254 Ditzingen, Germany*
[b]*University of Stuttgart, Graduate School of Excellence advanced Manufacturing Engineering (GSaME), Nobelstr. 12, 70569 Stuttgart, Germany*
[c]*TRUMPF Werkzeugmaschinen SE & Co. KG, Johann-Maus-Str. 2, 71254 Ditzingen, Germany*
[d]*University of Stuttgart, Institut für Strahlwerkzeuge (IFSW), Pfaffenwaldring 43, 70569 Stuttgart, Germany*

Abstract

Burr formation in laser cutting reduces the quality of the cut and causes the need for extra processing of parts. In this paper in-situ high-speed imaging has been used to gain insights into the impact of the melt dynamics in the cutting kerf on the formation of burr during laser cutting of metal. The images captured both, the melt dynamics in the kerf and the adhesion of the melt to the lower edge of the sheet. The results show that the formation of burr is due to the detachment of melt droplets from the cutting front to the edge of the cutting kerf, which then adhere to the rear side of the sheet. In addition, the adhesion of molten material at the lower side of the cutting front and the subsequent flow of the molten material along the lower edges of the cutting kerf also leads to formation of burr.

Keywords: laser cutting; high-speed imaging; melt dynamics; burr formation; cut kerf

1. Introduction

Burr formation during laser cutting negatively affects the quality of the cut and often necessitates additional post-processing. Burr formation is influenced by various process parameters, such as cutting speed, focal position, and pressure of assist gas. (Teixidor et al. 2014; Stoyanov et al. 2023; Stoyanov et al. 2020; Nabavi et al. 2024; Madić und Radovanović 2013; Levichev et al. 2020). An unfavorable combination of these process parameters can lead to an insufficient acceleration of the molten material, preventing it from overcoming adhesion forces at the lower surface of the workpiece. As a result, the melt may adhere at the bottom edge, solidify, and form burrs (Stoyanov et al. 2020).
While the influence of process parameters on burr formation has been widely studied, the role of melt dynamics within the cutting kerf has received limited attention (Teixidor et al. 2014; Stoyanov et al. 2023; Stoyanov et al. 2020; Nabavi et al. 2024; Madić und Radovanović 2013; Levichev et al. 2020).
Although some studies have used X-ray imaging to investigate the behavior of the melt at the cutting front (Lind et al. 2020; Lind et al. 2021), this method does not capture the melt flow along the cut edges. Consequently, the impact of the melt flow on the cut edges of the kerf on burr formation remains mostly unexplored.
A deeper understanding of these mechanisms is essential for improving process stability and cut quality. Therefore, this study aims to investigate the relationship between melt flow in the kerf and burr formation. To achieve this, in-situ high-speed imaging was used to capture the melt dynamics during laser cutting. The recordings enabled simultaneous observation of the melt flow within the kerf and the adhesion of molten material to the bottom edge of the sheet.

2. Experimental setup

The experiments were conducted using a 5-axis laser machine equipped with a multi-mode fiber laser. The process parameters are summarized in Tab. 1.

Table 1. Laser and process parameters used in the experiments

Beam source	Fiber laser (TruFiber 6000S)
Wavelength λ	1,070 nm
Beam Parameter Product BPP	2 mm•mrad
Laser Power P	3 kW
Focal diameter d_f	200 µm
Focal position	+ 5 mm
Focal diameter on top surface of the sheet metal	283 µm
Cutting speed v	1 m/min to 11 m/min
Stand of Distance SOD	10 mm
Cutting Gas	Nitrogen
Pressure of Cutting Gas	7 and 14 bar
Material	ASTM A36
Material thickness	1.5 mm

The cutting speed was varied from 1 m/min to 11 m/min which corresponds to the maximum cutting speed before an incomplete cut at 12 m/min. To investigate the dynamics of the melt in the cutting kerf, in-situ high-speed imaging was used. The experimental setup is shown in Fig. 1, displaying both front and side views.

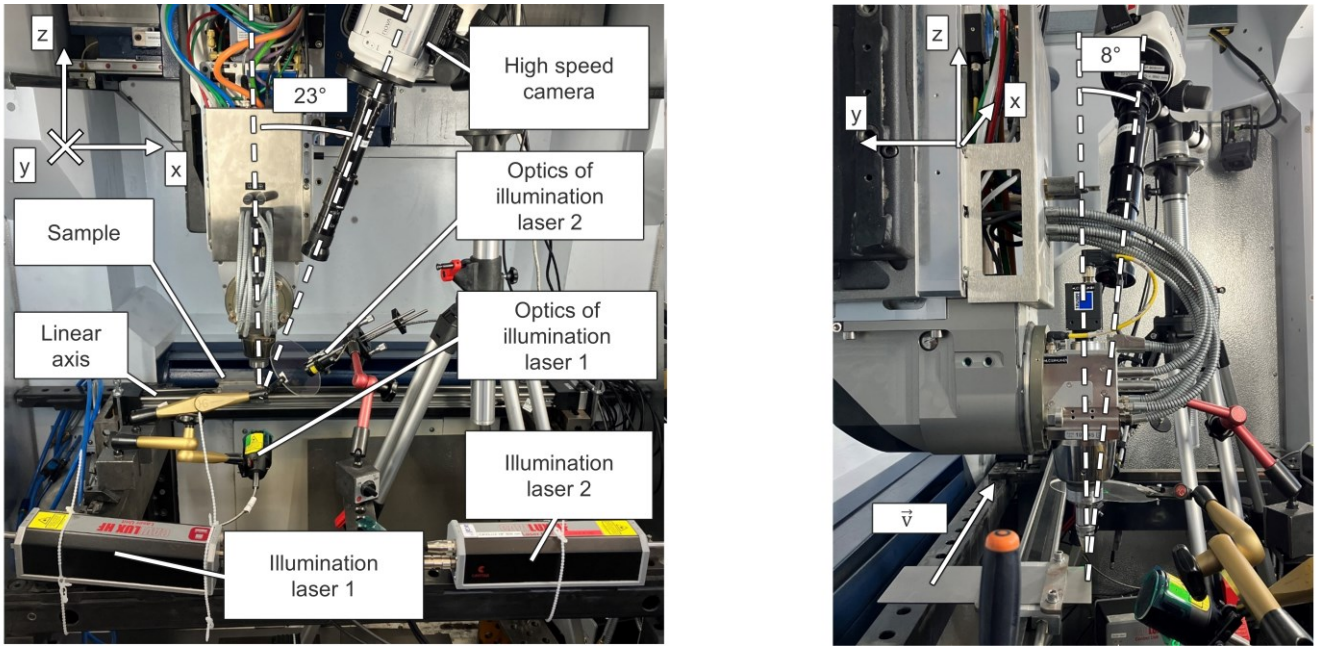

Fig. 1: Experimental setup for cutting the trials from different angles. Left: Side view. Right: Front view

To ensure a constant relative position between the camera and the processing zone, the sheet metal was mounted on a linear axis. The high-speed camera Nova S20 from Photron was positioned at an angle of 23° in the front view and 8° in the side view relative to the axis of the laser beam, as presented in Fig. 1. Two Cavilux lasers from Cavitar illuminated the observed interaction zone from the rear side of the sample by a wavelength of 808 nm, enabling clear visualization of the melt flow inside the kerf. An 850 nm short-pass filter was used to suppress the laser wavelength and thereby avoid

overexposure of the sensor. By using a short-pass filter, both thermal and laser-induced emissions could be observed simultaneously. The observation direction allowed simultaneous imaging of both the cut front, the cut edge and the potential burr formation. The sheet was mounted on a linear axis to ensure stable and repeatable movement during the cutting process. The sample was moved in positive x-direction.

3. Evaluation of the burr formation

Burr formation was evaluated by microscopic imaging of the cut samples. An Olympus MVX10 microscope equipped with an Olympus DP26 camera was used to image the edges of the samples. The evaluation of burr formation was based on visual inspection and subjective classification of the burr morphology. Characteristic features such as the presence of solidified melt films or individual adhering droplets were documented and correlated with the observed melt behavior in the high-speed video recordings. The images of the cut edges are shown in Fig. 2.

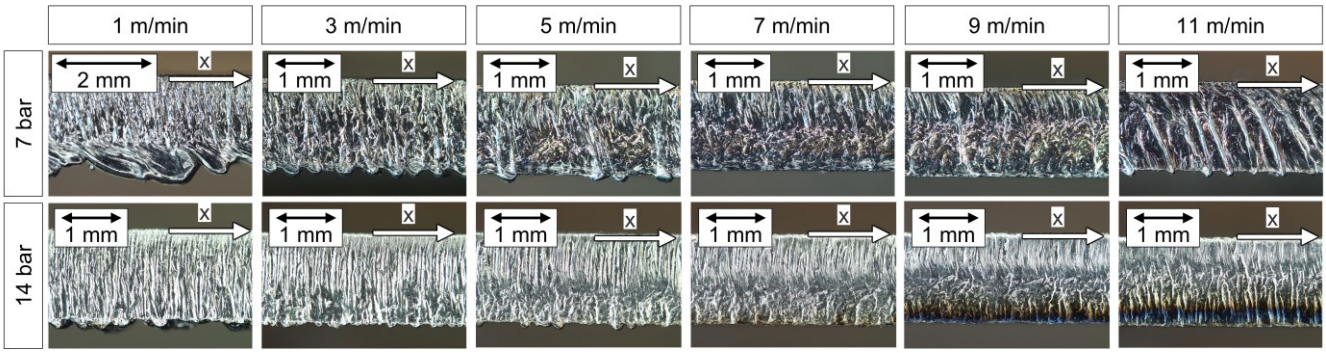

Fig. 2: Images of the cut edges

At a pressure of 7 bar, pronounced burr formation can be observed at low cutting speeds. At 1 m/min, large, droplet-shaped burrs are visible, oriented opposite to the cutting direction. The striation pattern appears irregular and inhomogeneous. Increasing the feed rate to 3 m/min leads to a slightly reduced but still pronounced burr formation, with similar inhomogeneous striations. At 5 m/min, burr formation further decreases, and the surface appearance remains comparable to 1 m/min. At cutting speeds of 7 m/min to 9 m/min, no significant burrs are visible, although the striation pattern remained irregular. At 11 m/min, burr formation increased again, comparable to the level at 5 m/min. In this case, melt droplets appeared to detach near the cut front and flow downward along the cut edge, solidifying at the bottom side of the sheet and forming burrs.

At a pressure of 14 bar, the overall burr formation is significantly reduced compared to 7 bar. At 1 m/min, only minor burrs are observed, and the striation pattern was uniform. At 3 m/min and 5 m/min, burr formation further decreased, and the upper part of the cut edge showed a homogeneous striation pattern, while the lower part became increasingly irregular, particularly at higher cutting speed. At 7 m/min and 9 m/min, only minimal burrs were visible, accompanied by increasing oxidation at the lower edge of the cut. At 11 m/min, the cut appearance remained nearly identical to that at 9 m/min, with very low burr formation and pronounced oxidation at the bottom of the kerf, which can be clearly identified by the blue colored surface.

4. Evaluation of the high speed video recordings

Fig. 3 shows time-averaged images extracted from high-speed videos of selected cutting trials. Each image represents the mean grey scale distribution over the course of a single cut. A general increase in image brightness is observed at higher cutting speeds. This may indicate increased thermal emission and, by implication, a larger amount of melt in the cutting front, potentially corresponding to a thicker melt film.

However, this interpretation remains a hypothesis, as the recorded grey scale values result from a superposition of thermal emission and reflected light from the illumination lasers. Consequently, it is not possible to clearly distinguish whether the increased brightness is solely due to thermal radiation from the melt.

Despite this uncertainty, a correlation is observed between higher grey scale values and reduced burr formation, as shown in Fig. 2. This may suggest that thicker melt films, if present, help suppress burr formation, possibly due to cohesive forces within the melt counteracting adhesion at the lower sheet edge. Additionally, the images recorded at $p = 14$ bar appear

noticeably brighter than those at p = 7 bar. However, this difference is attributed to slight variations in exposure settings during image acquisition and does not necessarily reflect an actual change in melt behavior.

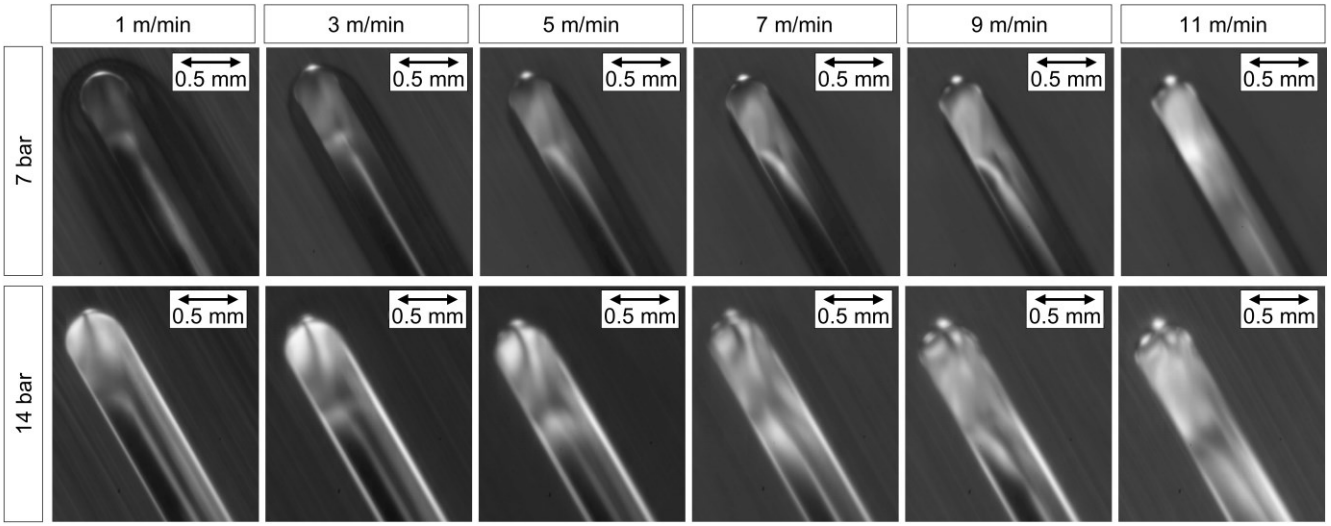

Fig. 3: Time-averaged images extracted from the high speed videos

Overall, the time-averaged images of Fig. 3 offer limited insight into the dynamics of the melt and their influence on burr formation. To better understand the underlying mechanisms, individual video frames are examined in the following, focusing on the process condition that exhibited the most pronounced burr formation: a gas pressure of 7 bar and a cutting speed of 1 m/min. Fig. 4 shows a sequence of selected frames from this trial.

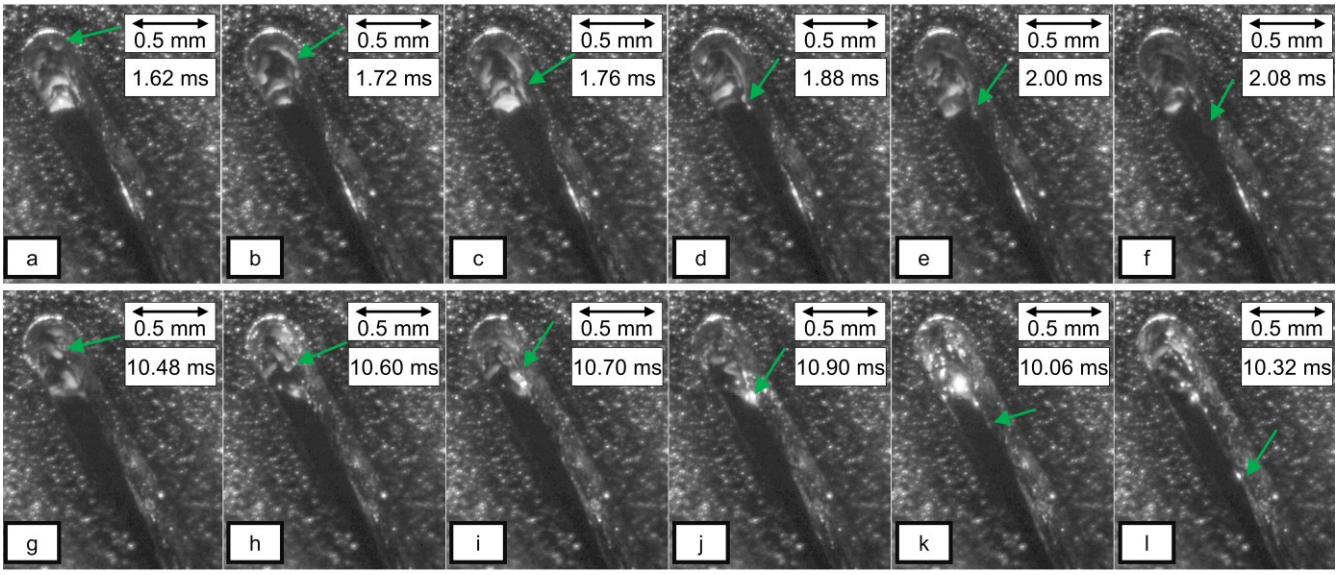

Fig. 4: Sequence of selected frames from the high speed video at p = 7 bar and a cutting speed of 1 m/min

The images reveal several instances of droplet detachment from the melt front, highlighted by the green arrow. In frames (a) to (f), such events occur near the upper edge of the kerf, where small volumes of molten material separate from the melt film. These droplets move downward along the kerf wall and are likely to solidify at the bottom edge, contributing to burr formation. However, similar detachment events can also be observed in the middle section of the cutting front, as seen in frames (g) to (l). This indicates that melt instabilities and droplet formation are not confined to a specific location but occur along various regions of the melt front. The spatially distributed nature of these events suggests a dynamic and stochastic process that may strongly influence the formation and distribution of burr.

5. Conclusion and outlook

The presented study demonstrates the link between melt dynamics and burr formation during laser cutting. For the first time, an experimental approach was implemented that enables simultaneous observation of the melt flow at the cutting front, along the kerf wall, and at the bottom edge where burr formation occurs. Within the considered parameters, the following key findings can be derived:

- Increased grey scale values in time-averaged images correlate with reduced burr formation. This may indicate the presence of thicker melt films, which could enhance cohesive forces within the melt and thereby reduce material attachment at the lower edge. Brighter regions in the images likely correspond to areas with a higher amount of melt and increased melt temperature, resulting in a thicker and more continuous melt film. However, this interpretation remains hypothetical due to the superimposed nature of thermal emission and reflected illumination light.
- Events of droplet detachment from the melt film were observed both at the upper edge and in the middle section of the cutting front.
- These events contribute to burr formation and occur in a spatially distributed, stochastic manner.

Further investigations should explore process strategies, such as pulsed cutting, that may promote the formation of thicker melt films. These may increase melt cohesion and help stabilize the flow, potentially reducing droplet detachment and burr formation.

Acknowledgements

This work was supported by the Landesministerium für Wissenschaft, Forschung und Kunst Baden-Württemberg (Ministry of Science, Research and the Arts of the State of Baden-Wurttemberg) within the Nachhaltigkeitsförderung (sustainability support) of the projects of the Exzellenzinitiative II.

References

Levichev, Nikita; Rodrigues, Gonçalo Costa; García, Alberto Tomás; Duflou, Joost R. (2020): Trim-cut technique for analysis of melt flow dynamics in industrial laser cutting machine. In: *Procedia CIRP* 95 (1), S. 858–863. DOI: 10.1016/j.procir.2020.01.157.

Lind, Jannik; Fetzer, Florian; Blazquez-Sanchez, David; Weidensdörfer, Jens; Weber, Rudolf; Graf, Thomas (2020): Geometry and absorptance of the cutting fronts during laser beam cutting. In: *Journal of Laser Applications* 32 (3), S. 32015. DOI: 10.2351/7.0000024.

Lind, Jannik; Hagenlocher, Christian; Blazquez-Sanchez, David; Hummel, Marc; Olowinsky, Alexander; Weber, Rudolf; Graf, Thomas (2021): Influence of the laser cutting front geometry on the striation formation analysed with high-speed synchrotron X-ray imaging. In: *IOP Conf. Ser.: Mater. Sci. Eng.* 1135 (1), S. 12009. DOI: 10.1088/1757-899X/1135/1/012009.

Madić, Miloš J.; Radovanović, Miroslav R. (2013): Identification of the Robust Conditions for Minimization of the HAZ and Burr in CO2 Laser Cutting. In: *FME Transactions* (41), S. 130–137.

Nabavi, Seyedeh Fatemeh; Farshidianfar, Anooshiravan; Dalir, Hamid (2024): An applicable review on recent laser beam cutting process characteristics modeling: geometrical, metallurgical, mechanical, and defect. In: *The International Journal of Advanced Manufacturing Technology* 130 (5-6), S. 2159–2217. DOI: 10.1007/s00170-023-12812-0.

Stoyanov, Stoyan; Petring, Dirk; Arntz-Schroeder, Dennis; Günder, Maurice; Gillner, Arnold; Poprawe, Reinhart (2020): Investigation on the melt ejection and burr formation during laser fusion cutting of stainless steel. In: *Journal of Laser Applications* 32 (2), S. 22068. DOI: 10.2351/7.0000074.

Stoyanov, Stoyan; Petring, Dirk; Piedboeuf, Frederik; Oliveira Lopes, Marcelo de; Schneider, Frank (2023): Numerical and experimental investigation of the melt removal mechanism and burr formation during laser cutting of metals. In: *Journal of Laser Applications* 35 (4), Artikel 042028, S. 43. DOI: 10.2351/7.0001182.

Teixidor, Daniel; Ciruana, Jordi; Rodriguez, Carles Armengol (2014): Dross formation and process parameters analysis of fiber laser cutting of stainless steel thin sheets. DOI: 10.1007/s00170-013-5599-0.